CETUC

Publicações em Antenas

Number 3 | April 2011

GO Shaping of Omnidirectional Dual-Reflector Antennas for a Prescribed Equi-Phase Aperture Field Distribution

Fernando José da Silva Moreira

Aluizio Prata Jr.

José Ricardo Bergmann

GRUPO DE ANTENAS

PUC RIO

Publicações em Antenas

Number 3 | April 2011

GO Shaping of Omnidirectional Dual-Reflector Antennas for a Prescribed Equi-Phase Aperture Field Distribution

Fernando José da Silva Moreira

Aluizio Prata Jr.

José Ricardo Bergmann

CRÉDITOS

Publisher:
MAXWELL / LAMBDA-DEE
Sistema Maxwell / Laboratório de Automação de Museus, Bibliotecas Digitais e Arquivos
http://www.maxwell.lambda.ele.puc-rio.br/

Editor:
Jose Ricardo Bergmann

Capa:
Ana Cristina Costa Ribeiro

GO Shaping of Omnidirectional Dual-Reflector Antennas for a Prescribed Equi-Phase Aperture Field Distribution

Fernando José da Silva Moreira, *Member, IEEE*, Aluizio Prata, Jr., *Member, IEEE*, and José Ricardo Bergmann, *Member, IEEE*

***Abstract*—A formulation is presented for shaping dual-reflector antennas designed to offer an omnidirectional coverage. The shaping procedure is based on geometrical optics (GO) principles and assumes a uniform phase distribution for the aperture field. Two distinct dual-reflector arrangements, based on the axis-displaced Cassegrain (ADC) and ellipse (ADE) configurations, are investigated. The GO shaping results are validated using the accurate analysis provided by the method-of-moments technique.**

***Index Terms*—Omnidirectional antennas, reflector antennas, reflector shaping.**

I. Introduction

REFLECTOR antennas are widely used in microwave and millimeter-wave communications and radar systems demanding large data rates. This is a consequence of their high efficiency capability, relative mechanical simplicity, and inherent broadband characteristics. All these features are ultimately related to their quasi-optical operation behavior. Usually reflector antennas are designed for maximum directivities (as in point-to-point microwave links), but some attention has recently been devoted to reflector arrangements providing omnidirectional coverage [1]–[9]. Among other uses, omnidirectional reflector antennas are useful as base-station radiators for point-to-multipoint radio links, such as local multipoint distribution services (LMDS).

The work available in the literature covers both classical reflector arrangements (i.e., geometries whose reflectors are generated by conic sections) [2], [7]–[9] and shaped reflectors [1], [3]–[6]. However, no study has yet been devoted to the synthesis of highly-efficient omnidirectional dual-reflector antennas, which are achieved by means of a uniform aperture illumination. On this light, the objective of this work is to present a simple and efficient dual-reflector shaping procedure based on geometrical optics (GO) principles. This procedure can be used to obtain an aperture illumination with uniform phase and polarization, and an arbitrary user-specified amplitude, starting from a prescribed circularly symmetric feed radiation (and some other pertinent geometrical parameters). The arbitrariness of the aperture field amplitude allows the application of the present GO shaping procedure to geometries aiming at maximum antenna directivity (i.e., by choosing a uniform amplitude distribution) or low sidelobe levels (i.e., by implementing a tapered amplitude distribution).

In the next section some basic geometrical features of omnidirectional dual-reflector antennas are briefly discussed. In Section III we derive a GO shaping algorithm, suited for producing an equi-phase aperture field. In Section IV we present two case studies of omnidirectional dual-reflector configurations shaped for uniform aperture illumination and maximum directivity (according to GO principles). Two additional case studies are investigated in the subsequent section, this time with a tapered amplitude distribution imposed over the antenna aperture to reduce the radiated sidelobe levels. All case studies discussed here are validated using accurate analyses based on the method of moments (MoM) technique, which accounts for all the electromagnetic effects present on the reflectors and feed structure. This work terminates with some brief conclusions.

II. Basic Geometrical Features

There are four different types of dual-reflector antennas capable of providing omnidirectional coverages, but those based on the classical axis-displaced Cassegrain (ADC) and axis-displaced ellipse (ADE) seem to be the most appropriate ones for yielding compact arrangements [8]. Such axially-symmetric arrangements are depicted in Figs. 1 and 2, respectively, together with some pertinent geometrical parameters. Inspection of these figures indicate that the most relevant difference between the ADC- and ADE-like configurations is that the principal ray (i.e., the ray leaving the antenna system focus, point O, along the symmetry axis and striking the subreflector at its vertex) meets the main reflector at its inner (outer) rim in the ADC (ADE) arrangement. The fundamental consequence of this is that, to a first order, the ADE-like reflector system provides a reversal of the feed illumination at the antenna aperture—a feature that can be successfully exploited by the antenna designer.

Among the various antenna geometrical parameters, it is useful to single out in Figs. 1 and 2 the width W_A of the antenna conical aperture, the main-reflector outer and inner projected diameters (D_M and D_B, respectively), the subreflector projected diameter D_S, the distance V_S from the reflector-system

Manuscript received October 5, 2005; revised September 5, 2006. This work was supported in part by CNPq, Brazil, under Projects 471750/2004-2 and 302749/2004-7, and in part by FAPERJ, Brazil, under Project E-26/171083/03.

F. J. da Silva Moreira is with the Department of Electronics Engineering of the Federal University of Minas Gerais, 30161-970 Belo Horizonte, MG, Brazil (e-mail: fernandomoreira@ufmg.br).

A. Prata, Jr., is with the Department of Electrical Engineering—Electrophysics, University of Southern California, Los Angeles, CA 90089-0271 USA.

J. R. Bergmann is with the Center for Telecommunications Studies of the Catholic University, 22453-900 Rio de Janeiro, RJ, Brazil.

Digital Object Identifier 10.1109/TAP.2006.888396

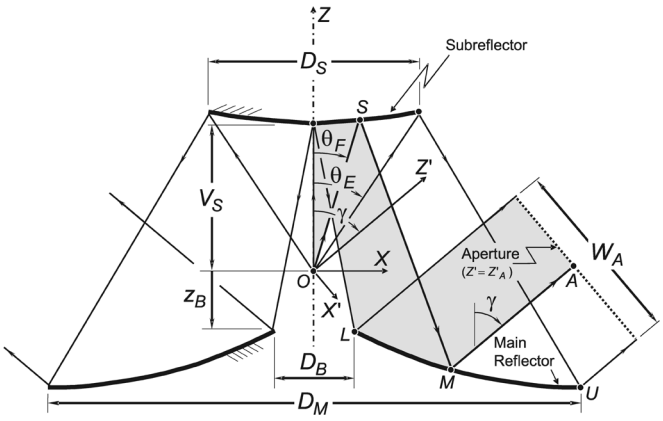

Fig. 1. Geometry of the ADC-like omnidirectional dual-reflector antenna.

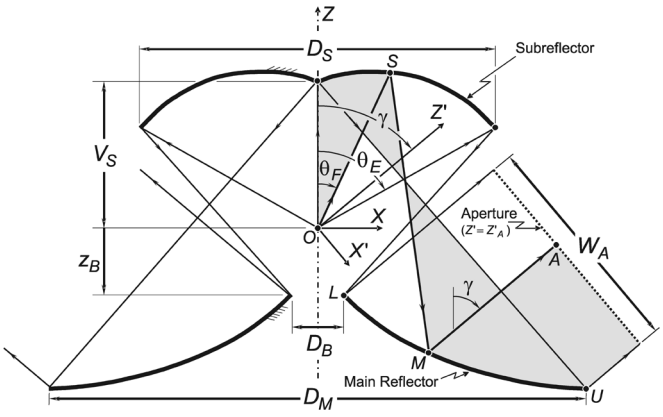

Fig. 2. Geometry of the ADE-like omnidirectional dual-reflector antenna.

focus O (which is also the origin of the coordinate systems used here) to the subreflector vertex, the z-coordinate z_B of the rim of the main-reflector central hole (i.e., the z-coordinate of point L), the subreflector edge angle θ_E, and the angle γ between the rays reflected by the main reflector and the symmetry axis. The angle γ corresponds to the direction of maximum directivity of the omnidirectional antenna radiation pattern in the elevation plane. Note that by making $\gamma = 0$ the present geometries reduce to the configurations described in [10]. Another important parameter is the path length ℓ_o, which is imposed to be constant for any ray traveling from the system focus O to the conical aperture surface at point A. Under a GO perspective, this constant path length imposes the desired uniform phase distribution over the antenna aperture.

III. GO Shaping Formulation

Many GO reflector-shaping algorithms have been developed since Galindo's pioneering work [11] but, for the task at hand, we present an alternative shaping procedure originally developed for directive circularly-symmetric dual-reflector antennas [12]. The procedure is similar to that in [13], with the relevant difference that Fermat's principle is directly imposed instead of Snell's law to treat the reflection at the subreflector surface.

Referring to Figs. 1 and 2, let $\overline{OSM}$ be the optical path length of an arbitrary ray that departs from O, reflects on the subreflector surface at S, and arrives at the main-reflector surface at point M, before continuing toward the antenna aperture. Such path length must then obey Fermat's principle (and, consequently, Snell's law at the reflecting point S), i.e., $\overline{OSM}$ must be stationary with respect to the feed-ray angle, namely θ_F. Consequently

$$\frac{d}{d\theta_F}\overline{OSM} = 0. \tag{1}$$

Recalling that

$$\overline{OSM} = r_F + \sqrt{(x_M - x_S)^2 + (z_M - z_S)^2} \tag{2}$$

where r_F is the distance from O to S, x_M and z_M are the coordinates of M, and

$$\begin{aligned} x_S &= r_F \sin\theta_F \\ z_S &= r_F \cos\theta_F \end{aligned} \tag{3}$$

are the coordinates of S, one can show from (1) that

$$\frac{dr_F}{d\theta_F} = \frac{r_F(x_M\cos\theta_F - z_M\sin\theta_F)}{\overline{OSM} - (x_M\sin\theta_F + z_M\cos\theta_F)} \tag{4}$$

which is the first-order differential equation to be solved for the reflector surfaces. In this work, the independent variable is assumed to be θ_F. Hence, in (4) there are three variables to be determined: the subreflector coordinate r_F and the main-reflector coordinates x_M and z_M.

The main-reflector coordinates x_M and z_M are obtained by applying the conservation of energy along a ray tube and by enforcing the desired constant path length ℓ_o from O to the aperture point A. However, to render simpler equations it is appropriate to define first an auxiliary tilted Cartesian coordinate system (the x', z' system depicted in Figs. 1 and 2) to describe the main-reflector coordinates, such that

$$\begin{aligned} x' &= x\cos\gamma - z\sin\gamma \\ z' &= x\sin\gamma + z\cos\gamma. \end{aligned} \tag{5}$$

Now, from Figs. 1 and 2 one observes that the equal path-length condition can be enforced by imposing

$$\ell_o = \overline{OSM} - z'_M + z'_A \tag{6}$$

where z'_M is the z'-coordinate of the main-reflector point M and z'_A is the constant (and predetermined) z'-coordinate of the antenna conical aperture surface. In practice, the value of z'_A is arbitrary, as long as it is sufficiently large to prevent the aperture

surface from intersecting the antenna symmetry axis. Substituting (2), (3), and (5) into (6), this last equation can be rewritten as

$$z'_M = \frac{x'_M\left[x'_M + 2r_F\sin(\gamma-\theta_F)\right] - (\ell_o - z'_A)(\ell_o - z'_A - 2r_F)}{2\left\{\ell_o - z'_A - r_F\left[1-\cos(\gamma-\theta_F)\right]\right\}}. \tag{7}$$

To determine the corresponding x'-coordinate of M (i.e., x'_M), conservation of energy is used [13]. However, as the ADE-like antenna provides the reversal of the feed illumination at the antenna aperture while the ADC-like antenna does not, a distinction must be made between the two geometries in the shaping algorithm. This can be accomplished by observing that, for the ADC-like configuration (Fig. 1), the conical ray tube emanating from O with semi-angle θ_F is mapped at the aperture with $x' \in [x'_L, x'_M]$, while for the ADE-like antenna (Fig. 2) the mapping occurs with $x' \in [x'_M, x'_U]$. In these equations, x'_L and x'_U are the x'-coordinates of the main-reflector points L and U, respectively, given by

$$\begin{aligned} x'_L &= (D_B/2)\cos\gamma - z_B\sin\gamma \\ x'_U &= x'_L + W_A. \end{aligned} \tag{8}$$

Hence, for the ADC- and ADE-like antennas, conservation of energy along the conical ray tube with vertex semi-angle θ_F requires that

$$\int_0^{\theta_F} F(\theta) r_F^2 \sin\theta d\theta = N \int_{x'_L}^{x'_M} P(x')\rho(x')dx' \tag{9}$$

and

$$\int_0^{\theta_F} F(\theta) r_F^2 \sin\theta d\theta = N \int_{x'_M}^{x'_U} P(x')\rho(x')dx' \tag{10}$$

respectively, where $F(\theta)$ is the circularly-symmetric feed power density, $P(x')$ is the desired aperture power density,

$$\rho(x') = x'\cos\gamma + z'_A\sin\gamma \tag{11}$$

is the radial distance from the symmetry axis to the antenna aperture, and

$$N = \left[\int_0^{\theta_E} F(\theta) r_F^2 \sin\theta d\theta\right] \Big/ \left[\int_{x'_L}^{x'_U} P(x')\rho(x')dx'\right] \tag{12}$$

is the normalization factor that assures that all the feed power intercepted by the subreflector is conserved at the antenna conical aperture.

Once x'_M and z'_M are determined from (6)–(12), (5) can be used to obtain x_M and z_M, which can be substituted into (4) to yield a first-order non-linear differential equation where the only unknown to be determined is r_F. The subreflector coordinate r_F can then be obtained by stepping θ_F from 0 to θ_E and numerically solving (4) using any one of the several widely available techniques, with the following initial condition (see Figs. 1 and 2):

$$r_F(\theta_F = 0) = V_S. \tag{13}$$

In the case studies discussed below, the fourth-order Runge-Kutta method [14] was employed to solve (4).

IV. Case Studies With Uniform Aperture Illumination

Before proceeding to the shaping and analysis of two case studies of omnidirectional dual-reflector antennas designed for maximum directivity, it is convenient to establish associated classical geometries to estimate the initial design parameters. Because of its applicability, hereinafter it is assumed that $\gamma = 90°$. Classical omnidirectional dual-reflector antennas with $\gamma = 90°$ are investigated in [8] and [9], where formulas and results for geometries with relatively large radiation efficiencies are presented. So, from [8] and [9] we have established, for the case studies below, the classical ADC and ADE arrangements depicted in Figs. 3(a) and 4(a), respectively, together with appropriate optical paths (from O to the antenna aperture) and feed geometry (a coaxial horn with $R_i = 0.45\lambda$ and $R_e = 0.9\lambda$, providing a subreflector-edge taper of about 13 dB without including path-length loss). The coaxial horn was employed for having an omnidirectional radiation pattern with a null at $\theta = 0$ and for providing a desirable vertical polarization [2], [5]–[9]. Alternatively, conical horns solely excited by the TE_{01} or TM_{01} mode can be used, providing horizontal or vertical polarization, respectively [3]. Relevant geometrical and electrical characteristics of these antennas are summarized in Table I, including the maximum directivity D_o at $\theta = 90°$ and the radiation efficiency (Eff. %) with respect to a uniform cylindrical aperture and accounting for spilover losses.

The omnidirectional radiation patterns of the antennas, computed by two methods, are depicted in Figs. 3(b) and 4(b), respectively. For the aperture field analysis method (ApM), based on the GO aperture field, the following model was adopted for the field radiated by the TEM coaxial-horn feed [8], [9]

$$\begin{aligned} \vec{E}_F(\vec{r}_F) &= \left[\frac{J_0(kR_i\sin\theta_F) - J_0(kR_e\sin\theta_F)}{\sin\theta_F}\right]\frac{e^{-jkr_F}}{r_F}\hat{\theta}_F \\ \vec{H}_F(\vec{r}_F) &= \frac{1}{\eta}\hat{r}_F \times \vec{E}_F(\vec{r}_F) \end{aligned} \tag{14}$$

where k and η are the free-space wavenumber and wave impedance, respectively, $J_0(x)$ is the zero order Bessel function, and $R_i = 0.45\lambda$ and $R_e = 0.9\lambda$ are the internal and external radii of the adopted coaxial horn aperture, respectively. Equation (14) is simply the radiation field of a coaxial aperture mounted on an infinite perfect electric conductor plane and illuminated by the TEM mode of the corresponding coaxial waveguide [15], and satisfactorily represents the main

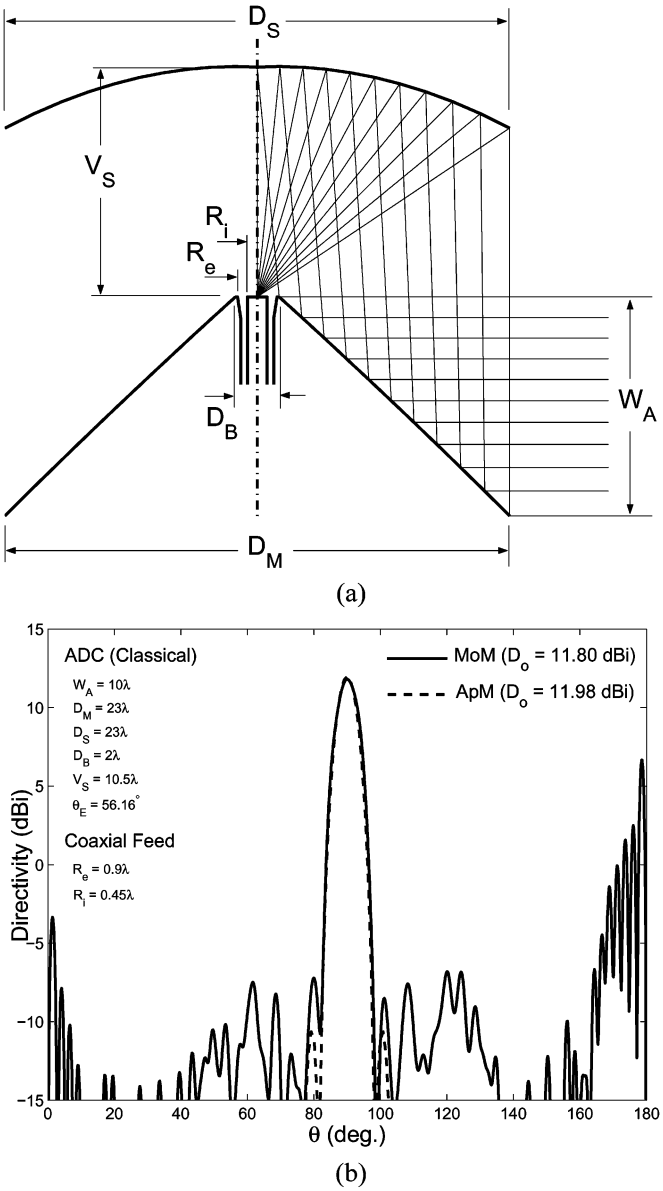

Fig. 3. Classical omnidirectional ADC antenna: (a) geometry and (b) radiation pattern.

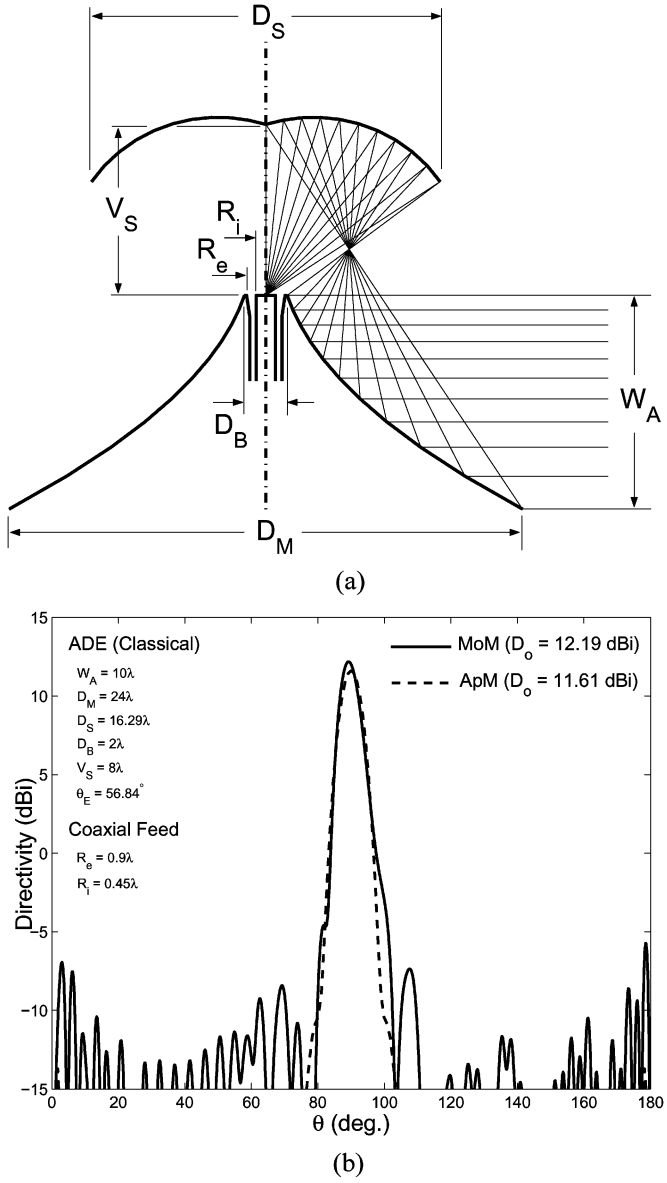

Fig. 4. Classical omnidirectional ADE antenna: (a) geometry and (b) radiation pattern.

lobe of the actual feed radiation pattern [8]. Furthermore, the MoM [16] results shown in Figs. 3(b) and 4(b) account for all electromagnetic field effects, including interactions between the reflector and horn structures, which explains the relatively large sidelobe levels observed.

To demonstrate the method presented in this work, the GO shaping formulation of Section III was applied to the above two classical reflector systems to yield maximum-directivity configurations [i.e., geometries with constant aperture power density $P(x')$], while maintaining the same values of W_A, γ, D_B, V_S, z_B, and θ_E of their classical counterparts. The feed radiation model of (14) was used to specify the circularly-symmetric feed power density in (9), (10), and (12) as

$$F(\theta_F) = \frac{\left|\vec{E}_F(\vec{r}_F)\right|^2}{2\eta}. \tag{15}$$

It is also important to mention that, as $\gamma = 90^\circ$ and $z_B = 0$ for the present case studies, $x'_L = 0$ and $x'_U = W_A$ according to (8), while we arbitrarily set $\rho = z'_A = 10\lambda$ in (11). The shaped reflector surfaces of the ADC- and ADE-like configurations are depicted in scale (using solid lines) in Figs. 5(a) and 6(a), respectively, together with their classical counterparts (dashed lines). The radiation patterns are those of Figs. 5(b) and 6(b), respectively, which depict the directivity improvement provided by the shaping procedure. Relevant characteristics of these two shaped reflector systems are also listed in Table I.

V. Case Studies With Tapered Amplitudes

The results of Figs. 5(b) and 6(b) indicate that the increase in directivity, provided by the uniform illumination of the cylindrical antenna aperture, comes with a sidelobe level increase, as expected from aperture radiation theory. Since this may be undesirable in some applications, in this section we consider

TABLE I
CHARACTERISTICS OF THE OMNIDIRECTIONAL DUAL-REFLECTOR ANTENNAS OF FIGS. 3–6, 9, AND 10

Antenna Charact.		ADC Clas.	ADC Unif. Apert.	ADC Taper. Apert.	ADE Clas.	ADE Unif. Apert.	ADE Taper. Apert.
$W_A(\lambda)$		10	10	10	10	10	10
$\gamma(^\circ)$		90	90	90	90	90	90
$D_M(\lambda)$		23	21.76	22.59	24	21.52	22.79
$D_S(\lambda)$		23	22.33	22.77	16.29	16.77	16.52
$D_B(\lambda)$		2	2	2	2	2	2
$V_S(\lambda)$		10.5	10.5	10.5	8	8	8
$z_B(\lambda)$		0	0	0	0	0	0
$\theta_E(^\circ)$		56.16	56.16	56.16	56.84	56.84	56.84
D_o	MoM	11.80	12.46	12.35	12.19	12.26	12.73
(dBi)	ApM	11.98	12.83	12.34	11.61	12.83	12.30
Eff.	MoM	76.3	88.8	86.6	83.4	84.8	94.5
(%)	ApM	79.6	96.7	86.4	73.0	96.7	85.6

the possibility of shaping the reflector surfaces for a tapered amplitude distribution at the antenna aperture to reduce sidelobe levels. Many tapered amplitude distributions have been proposed for the blocked circular apertures commonly encountered in highly directive circularly-symmetric dual-reflector systems, and all of them can be readily extended to the present omnidirectional configurations. On this light it is relevant to mention the authoritative studies conducted by Ludwig [17]. Based on [17], here we propose an alternative amplitude distribution, which is tapered toward the aperture rims to provide lower sidelobes, and flat in the middle of the aperture to minimize the directivity loss due to tapering.

The proposed tapered aperture power density distribution is given in terms of x' as

$$P(x')=\begin{cases}(\Delta_1)^{\alpha_1}\left[1+(\alpha_1/\beta_1)(1-\Delta_1)\right]^{\beta_1}, & x'_L<x'<x'_1\\ 1, & x'_1<x'<x'_2\\ (\Delta_2)^{\alpha_2}\left[1+(\alpha_2/\beta_2)(1-\Delta_2)\right]^{\beta_2}, & x'_2<x'<x'_U\end{cases} \tag{16}$$

where x' is the x'-coordinate of the aperture point A (see Figs. 1 and 2)

$$\begin{aligned}\Delta_1&=\chi_1+(1-\chi_1)\,(x'_L-x')\,/\,(x'_L-x'_1)\\ \Delta_2&=\chi_2+(1-\chi_2)\,(x'_U-x')\,/\,(x'_U-x'_2)\end{aligned} \tag{17}$$

and the parameters α_i, β_i, χ_i, and x'_i (with $i=1,2$) control the tapered distribution near x'_L ($i=1$) and x'_U ($i=2$). Note that for the present case studies $x'_L=0$ and $x'_U=W_A$. Fig. 7 illustrates the typical behavior of (16), for the particular case of $\alpha_1=\alpha_2=\beta_1=3$, $\beta_2=1$, $\chi_1=0$, $\chi_2=0.5$, $x'_L=0$, and $x'_U=10$.

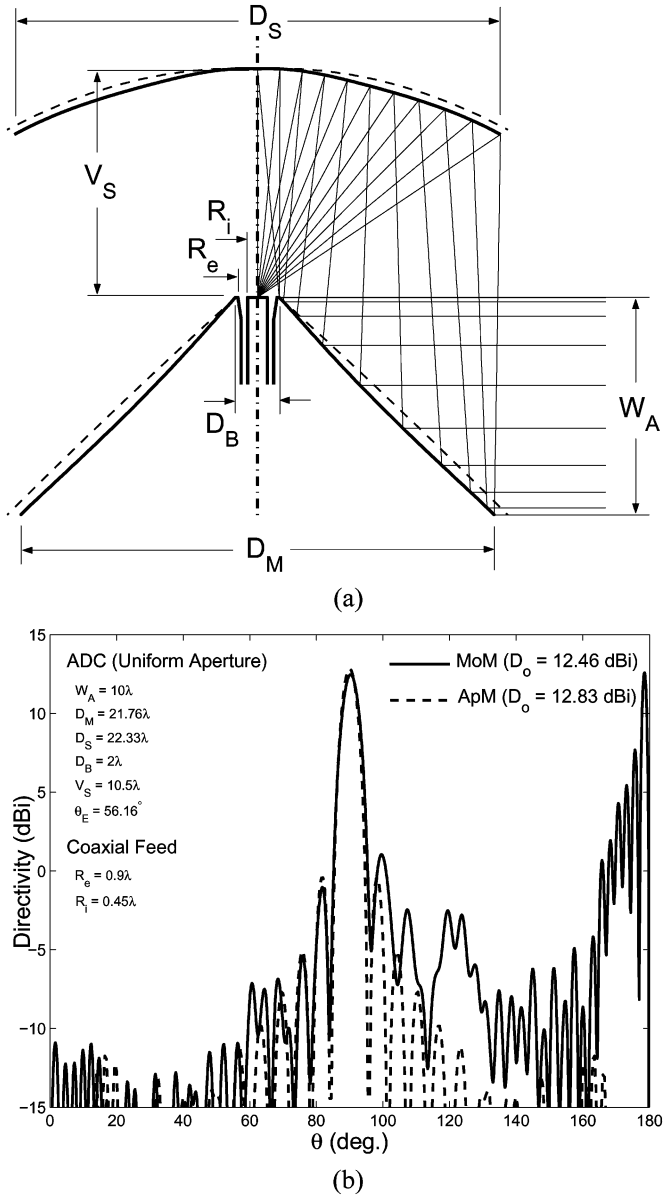

Fig. 5. Omnidirectional ADC-like antenna shaped for a uniform aperture illumination: (a) geometry (with the classical geometry of Fig. 3 in dashed lines) and (b) radiation pattern.

The distribution given by (16) has some interesting features. Its first derivative is zero at $x'=x'_1$ and $x'=x'_2$, yielding a smooth transition between the tapered and flat regions, which consequently reduces the associated diffraction effects. Besides, $\chi_1=0$ imposes $P(x'_L)=0$, which is the correct choice for shaping ADC-like dual-reflector systems. That is required because the scattering from the subreflector tip, which is directed toward the main-reflector rim L, produces zero aperture power density (according to GO principles). For the ADE-like configurations one must choose $\chi_2=0$, which yields $P(x'_U)=0$ instead.

The shaping of the tapered-aperture omnidirectional antennas were conducted exactly as discussed in Section IV, but with $P(x')$ given by (16) instead. The parameters of (16) were chosen

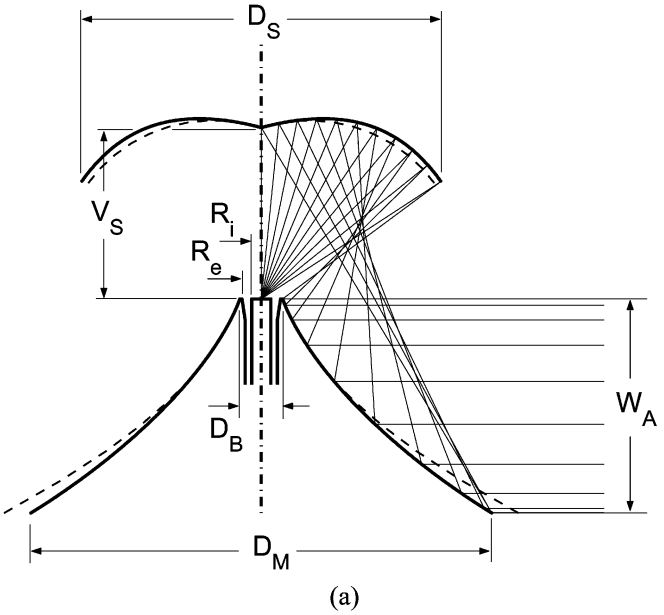

(a)

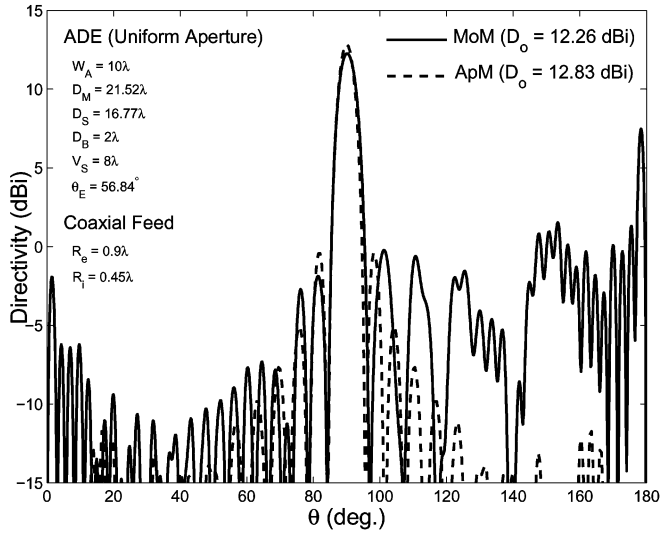

(b)

Fig. 6. Omnidirectional ADE-like antenna shaped for a uniform aperture illumination: (a) geometry (with the classical geometry of Fig. 4 in dashed lines) and (b) radiation pattern.

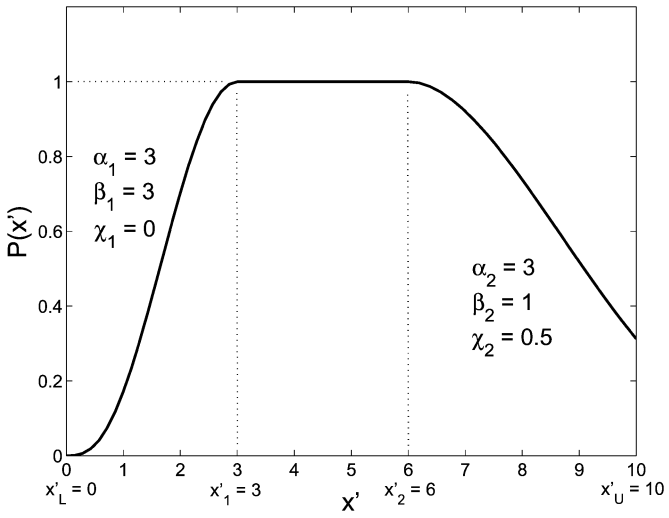

Fig. 7. Proposed tapered aperture power density.

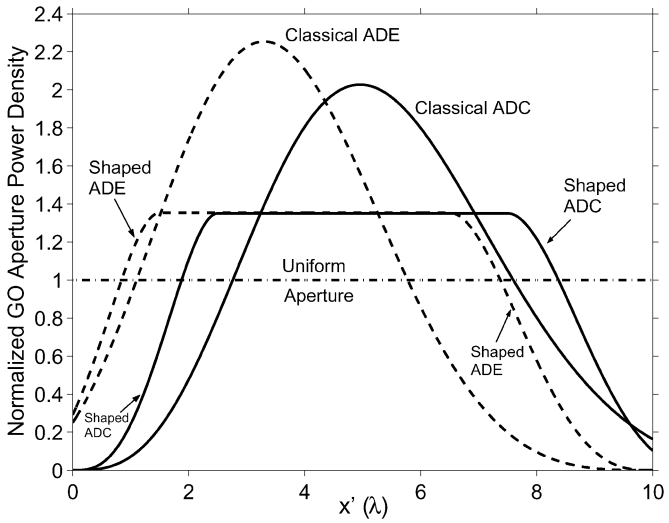

Fig. 8. Normalized aperture power densities of the several antenna geometries investigated.

based on the results of Figs. 3–6. One observes from those radiation patterns that the omnidirectional configurations shaped for a uniform aperture have considerably larger sidelobe levels in the region $90° < \theta \leq 180°$, when compared with their classical counterparts. So, without any attempt to optimize the parameters of (16), the tapered illuminations were arbitrarily specified to approximately resemble the aperture illuminations of their classical counterparts near $x' = x'_L$ and $x' = x'_U$, while providing a relatively wide flat region $(x'_2 - x'_1 = 5\lambda)$ to improve the antenna directivity. For the ADC-like configuration we have chosen $\alpha_1 = \alpha_2 = 3$, $\beta_1 = \beta_2 = 1$, $\chi_1 = 0$, $\chi_2 = 0.29$, $x'_1 = 2.5\lambda$, and $x'_2 = 7.5\lambda$. In turn, for the ADE-like antenna we have selected $\alpha_1 = \alpha_2 = 3$, $\beta_1 = \beta_2 = 1$, $\chi_1 = 0.43$, $\chi_2 = 0$, $x'_1 = 1.5\lambda$, and $x'_2 = 6.5\lambda$. For comparison, Fig. 8 depicts these GO aperture power densities for identical feed radiated power.

The ADC- and ADE-like shaped geometries, and the corresponding radiation patterns, are illustrated in Figs. 9 and 10, respectively, while some important characteristics are listed in Table I. Essentially, one observes that these configurations provide considerably lower sidelobe levels when compared with their uniform-aperture counterparts (Figs. 5 and 6), while still yielding directivities considerably higher than those of the classical configurations, as desired. Furthermore, one observes from Fig. 10(b) that the ADE-like shaped antenna ended up with a directivity larger than that of the uniform-aperture antenna of Fig. 6. The cause for this has not been further investigated, but it could be associated with second-order effects related to the coupling between the sub- and main-reflectors.

Finally, by comparing the antenna geometries in Figs. 3–6, 9, and 10 one observes that, for the shaped-reflector arrangements, the specified aperture power density forces an additional redistribution of the energy toward the aperture edge. So, at the lower aperture region, the required ray mapping brings the main-reflector surface close to the symmetry axis (z-axis), yielding a

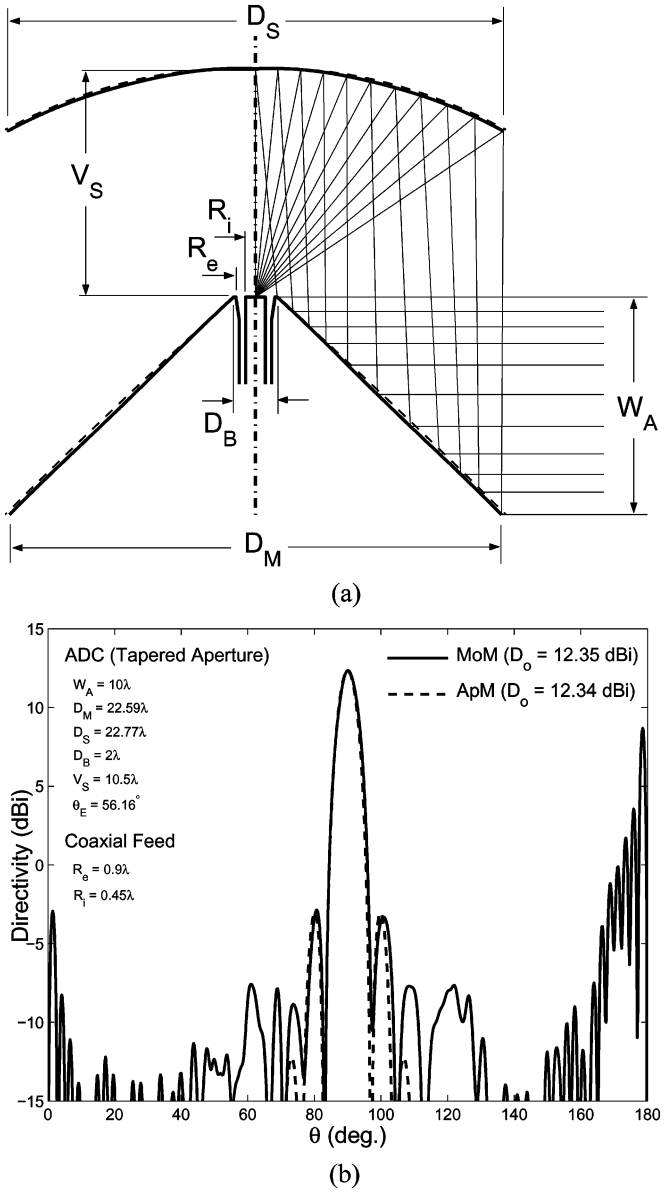

Fig. 9. Omnidirectional ADC-like antenna shaped for a tapered aperture illumination: (a) geometry (with the classical geometry of Fig. 3 in dashed lines) and (b) radiation pattern.

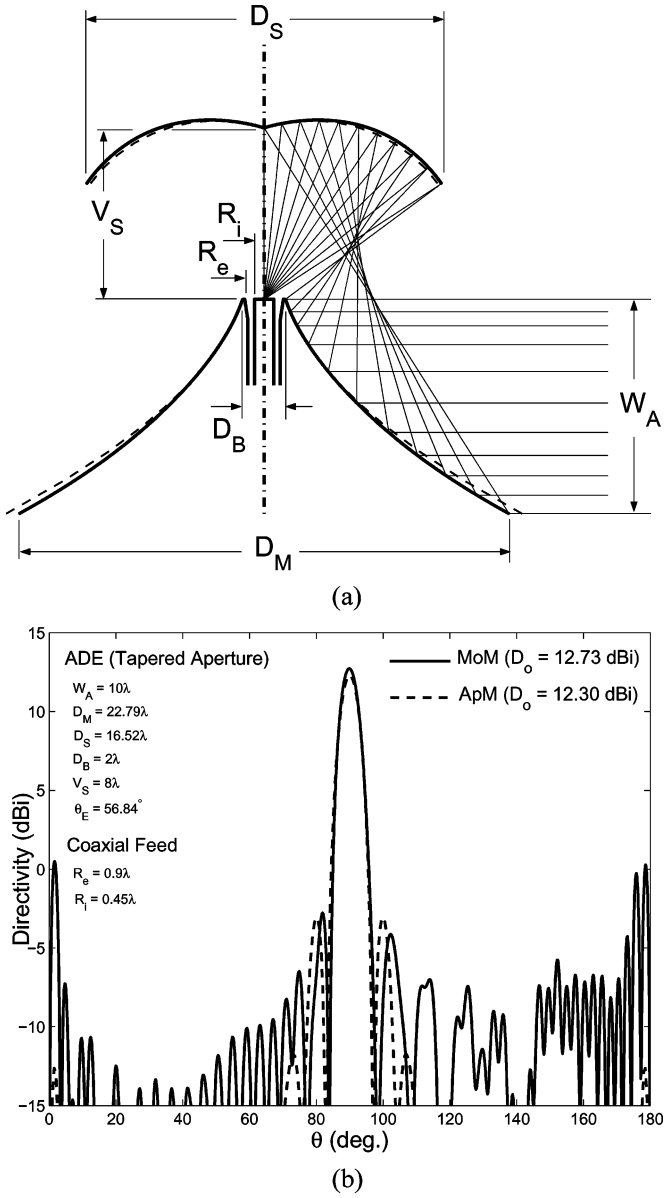

Fig. 10. Omnidirectional ADE-like antenna shaped for a tapered aperture illumination: (a) geometry (with the classical geometry of Fig. 4 in dashed lines) and (b) radiation pattern.

slightly smaller main-reflector diameter D_M, as listed in Table I. Therefore, besides the gain and sidelobe improvements, the reflector shaping also provides a small reduction in the volume of the cylinder that encloses the omnidirectional dual-reflector antenna.

VI. Conclusion

A GO shaping procedure was developed for dual-reflector antennas, whose axially-symmetric surfaces are suited for omnidirectional coverage. It was assumed that the GO field has a uniform phase on the aperture conical surface, imposed by an equal path length from the geometrical focus of the dual-reflector system to the conical aperture, while the field amplitude is arbitrarily specified by the antenna designer. The performance of the proposed GO shaping procedure was demonstrated on two different reflector configurations, derived from the classical ADC and ADE arrangements. Case-study antennas with uniform and tapered amplitudes were synthesized and their performances verified using accurate MoM analyses.

References

[1] A. P. Norris and W. D. Waddoup, "A millimetric wave omnidirectional antenna with prescribed elevation shaping," in *Proc. ICAP—4th Int. Conf. Antennas and Propagation*, 1985, pp. 141–145.

[2] M. Orefice and P. Pirinoli, "Dual reflector antenna with narrow broadside beam for omnidirectional coverage," *Electron. Lett.*, vol. 29, no. 25, pp. 2158–2159, Dec. 9, 1993.

[3] P. Besso, R. Bills, P. Brachat, and R. Vallauri, "A millimetric wave omnidirectional antenna with cosecant squared elevation pattern," in *Proc. ICAP—10th Int. Conf. Antennas and Propagation*, 1997, vol. 1, pp. 448–451.

[4] H. B. Abdullah, "A prototype Q-band antenna for mobile communication systems," in *Proc. ICAP—10th Int. Conf. Antennas and Propagation*, 1997, vol. 1, pp. 452–455.

[5] J. R. Bergmann, F. J. V. Hasselmann, and M. G. C. Branco, "A single-reflector design for omnidirectional coverage," *Microwave Opt. Tech. Lett.*, vol. 24, no. 6, pp. 426–429, Feb. 14, 2000.
[6] A. G. Pino, A. M. A. Acuña, and J. O. R. Lopez, "An omnidirectional dual-shaped reflector antenna," *Microw. Opt. Tech. Lett.*, vol. 27, no. 5, pp. 371–374, Dec. 5, 2000.
[7] J. R. Bergmann and F. J. S. Moreira, "An omni directional ADE reflector antenna," *Microwave Opt. Tech. Lett.*, vol. 40, no. 3, pp. 250–254, Feb. 5, 2004.
[8] F. J. S. Moreira and J. R. Bergmann, "Classical axis-displaced dual-reflector antennas for omnidirectional coverage," *IEEE Trans. Antennas Propag.*, vol. 53, no. 9, pp. 2799–2808, Sep. 2005.
[9] J. R. Bergmann and F. J. S. Moreira, "Simple design equations for omnidirectional axis-displaced dual-reflector antennas," *Microwave Opt. Tech. Lett.*, vol. 45, no. 2, pp. 159–163, Apr. 20, 2005.
[10] F. J. S. Moreira and A. Prata, Jr., "Generalized classical axially symmetric dual-reflector antennas," *IEEE Trans. Antennas Propag.*, vol. 49, no. 4, pp. 547–554, Ap. 2001.
[11] V. Galindo, "Design of dual-reflector antennas with arbitrary phase and amplitude distributions," *IEEE Trans. Antennas Propag.*, vol. AP-12, no. 4, pp. 403–408, Jul. 1964.
[12] A. Prata, Jr., Lecture Notes of the Graduate Course EE578—Reflector Antennas Dept. of Electrical Engineering-Electrophysics, Univ. Southern California, Spring 1995.
[13] J. J. Lee, L. I. Parad, and R. S. Chu, "A shaped offset-fed dual-reflector antenna," *IEEE Trans. Antennas Propag.*, vol. AP-27, no. 2, pp. 165–171, Mar. 1979.
[14] F. B. Hildebrand, *Introduction to Numerical Analysis*, 2nd ed. New York: Dover., 1987.
[15] R. F. Harrington, *Time-Harmonic Electromagnetic Fields*. New York: McGraw Hill, 1961.
[16] J. R. Mautz and R. F. Harrington, An Improved E-Field Solution for a Conducting Body of Revolution Dept. Electrical and Computer Engineering, Syracuse Univ., Tech. Rep. TR-80-1, 1980.
[17] A. C. Ludwig, "Low sidelobe aperture distributions for blocked and unblocked circular apertures," *IEEE Trans. Antennas Propag.*, vol. AP-30, no. 5, pp. 933–946, Sep. 1982.

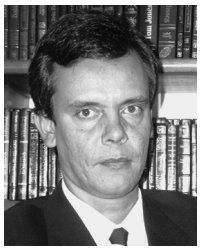

Fernando José da Silva Moreira (S'89–M'98) was born in Rio de Janeiro, Brazil, in 1967. He received the B.S. and M.S. degrees in electrical engineering from the Catholic University, Rio de Janeiro, Brazil, in 1989 and 1992, respectively, and the Ph.D. degree in electrical engineering from the University of Southern California, Los Angeles, in 1997.

Since 1998, he has been with the Department of Electronics Engineering of the Federal University of Minas Gerais, Belo Horizonte, Brazil, where he is currently an Associate Professor. His research interests are in the areas of electromagnetics, antennas and propagation. He has authored or coauthored over 70 journal and conference papers in these areas.

Dr. Moreira is a member of Eta Kappa Nu and the Brazilian Microwave and Optoelectronics Society.

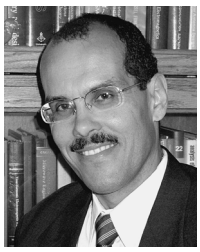

Aluizio Prata, Jr. (S'84–M'90) was born on March 18, 1954 in Uberaba, Brazil. He received the B.S. degree from the University of Brasilia, Brasilia, Brazil, in 1976, the M.S. degree from the Pontifical Catholic University of Rio de Janeiro, Rio de Janeiro, Brazil, in 1979, the M.S.E.E. degree from the California Institute of Technology, Pasadena, in 1984, and the Ph.D. from the University of Southern California, in 1990, all in electrical engineering.

From 1979 to 1983, he was with the Telebras Research and Development Center, Brazil, working on the design and construction of satellite earth station antennas. While at the California Institute of Technology he designed and implemented one of the first operational neural computers. Currently, he is an Associate Professor at the University of Southern California, working with applied electromagnetics. He is coauthor of the widely used PC interactive reflector-antenna design software RASCAL, currently with more than 1000 free copies distributed worldwide. He has been a Consultant for numerous aerospace companies, and has authored or coauthored over eighty articles, patents, and symposium papers.

Dr. Prata is a member of Sigma Xi, Eta Kappa Nu, and is an eminent member of Tau Beta Pi. He was a member of the steering committee of the 1995 IEEE Antennas and Propagation Society (APS) International Symposium, was the 1996 Chair of the Los Angeles Chapter of the IEEE APS (the Chapter won the 1996 Best Worldwide Chapter Award), and was the Vice Chair of the 2000 IEEE International Conference on Phased Array Systems and Technology. He is also the USC faculty advisor for the IEEE student chapter.

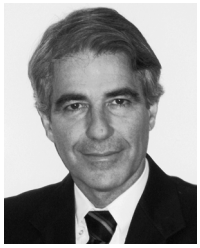

José Ricardo Bergmann (M'88) received the Electrical Engineering degree from the Universidade Federal do Rio Grande do Sul, Brazil, in 1975, the M.Sc. degree in electrical engineering from Instituto Militar de Engenharia, Brazil, in 1979, and the Ph.D. degree in electrical engineering from Queen Mary College, University of London, London, U.K., in 1986.

Currently, he is an Associate Professor and Head of the Antenna Group of the Center of Telecommunications Studies (CETUC) at the Catholic University of Rio de Janeiro, Brazil, where he has been Associate Vice President for Academic Affairs Research and Post Graduate of the Catholic University of Rio de Janeiro since 1998. His research interests comprise numerical modeling, synthesis and analysis of reflector systems.

Dr. Bergmann was Vice-President and President of the Brazilian Microwave and Optoelectronics Society (SBMO) from 1996 to 2000.